Journal of Molecular Liquids 345 (2022) 117907

Contents lists available at ScienceDirect

Journal of Molecular Liquids

journal homepage: www.elsevier.com/locate/molliq

Lateral organization of biomimetic cell membranes in varying pH conditions

Emilia Krok *, Agnieszka Batura, Madhurima Chattopadhyay, Hanna Orlikowska, Lukasz Piatkowski *

Poznan University of Technology, Faculty of Materials Engineering and Technical Physics, Institute of Physics, Piotrowo 3, 60-965 Poznan, Poland

ARTICLE INFO

Article history:
Received 1 September 2021
Revised 11 October 2021
Accepted 19 October 2021
Available online 22 October 2021

Keywords:
Biomimetic cell membranes
Supported lipid bilayers
pH
Phospholipids
Lipid domains

ABSTRACT

Many studies have been devoted to investigation of phase separation and formation of lipid domains, which play crucial role in many biological processes. Here we present a complex study on the formation, dynamics, and stability of the phase-separated supported lipid membranes under varying pH conditions. The size and distribution of liquid-ordered (L_o) phase domains were investigated in a wide range (1.7–9.0) of buffer pH values and a strong correlation was found between the size of the L_o domains and pH of the buffer hydrating the lipid bilayer. Interestingly, the dynamics of lipids composing both L_o and L_d phase are insensitive to the pH of the buffer. Our findings demonstrate that by varying pH of the environment one can induce formation of domains with a specific size and shape without any external modification of the solid support or altering the membrane composition. Finally, we show that the architecture of the lipid membrane is stable even upon replacement of the aqueous medium with the buffer of neutral pH. Consequently, this method of patterning of L_o phase domains in biomimetic membranes is applicable to the studies involving binding of proteins or incorporation of other pH-sensitive molecules.

1. Introduction

Biological membranes play a key role in the functioning of the cells. They are responsible for protecting the cell from changing external factors in the process called homeostasis. Moreover, they allow transportation of the ions and molecules such as glucose, amino acids, and lipids inside and outside the cell. The presented by Singer and Nicholson fluid mosaic model [1] is still the most accurate model describing the cell membrane. It proposes that cell membrane is composed of different types of lipids, forming more or less randomly organized fluid, in which there are embedded various components such as cholesterol, proteins, and carbohydrates. Sphingolipids and cholesterol form more organized micro- and nanoscopic domains, that are floating in the sea of phospholipids [2]. Sphingolipids with their long and saturated acyl chains allow the cholesterol to tightly intercalate with them, forming the liquid-ordered (L_o) phase [3]. On the other hand, unsaturated phospholipids are more loosely packed due to the structure of their acyl chains and are forming a liquid disordered (L_d) phase.

The lateral segregation in the membrane and compartmentalization by lipid domains are strongly related to many biological processes occurring in the body such as protein sorting [4], ion-channel regulation [5,6], signaling [7,8], membrane trafficking [9,10], organization of cytoskeleton [11,12] and pathogen entry [13,14]. Moreover, cholesterol- and sphingomyelin-rich domains are connected with the binding of toxins and their penetration inside the cell, as well as they are suggested to create the microenvironment promoting the prion formation and aggregation of amyloids [15]. The importance of the lipid domains led to the studies on how to manipulate their size and shape and questions as to the relations between size, distribution and the density of the domains with other membrane parameters such as diffusion coefficient or rigidity. So far the membrane structure was altered by changing its composition [16–19], the composition of the aqueous environment [20], the addition of lineactants [21], nucleation and spinodal decomposition processes [22], or applying different temperature and cooling speed during lipid bilayer formation [23].

One of the factors that affect the biological cell membranes is the change of the pH inside the cell as well as in the surrounding environment. The variations in the concentration of H^+ and OH^- ions, that occur outside the cell are responsible for the functioning of the cell, regulating its mobility [24,25] and deformation [26,27]. The internal changes of pH in the cells take part in the signaling mechanism of many cellular processes such as regulation of the cell cycle [28], proliferation [29], differentiation [30], and cell apoptosis [31]. The patterning of pH occurring within the cell plays

* Corresponding author.
E-mail addresses: emilia.krok@put.poznan.pl (E. Krok), lukasz.j.piatkowski@put.poznan.pl (L. Piatkowski).

https://doi.org/10.1016/j.molliq.2021.117907
0167-7322/

a key role in the organization of the cytoskeleton [32] and regulates the migration of its components [33]. The abnormal increase in intracellular and decrease in extracellular pH are connected with the mutation of cancer cells and tumor progression [34]. Clearly, the understanding of the influence of pH on biological cell membranes has become of great interest to biophysicists, biologists, and biochemists.

The investigation of lipid membranes in native form is difficult due to the complexity of the living cells as well as all the chemical, biological and physical processes that can alter the studied properties. The changes in the structure and dynamics of lipid membranes upon exposure to different pH conditions were checked so far on the systems such as supported black lipid membranes [35], liposomes [36], or single component supported lipid bilayers (SLBs). However, due to the higher complexity of lipid membranes exhibiting phase separation than those comprised of only one type of lipids, the studies on the behavior of L_o lipid domains under varying pH conditions so far were not addressed in detail.

To understand the behavior of the cell membranes under varying pH conditions we used supported lipid bilayers (SLBs), which mimic well the natural cell membranes [37]. Here we show how phase-separated membranes behave under a wide range of environmental pH 1.7–9.0. We observed that the structure of lipid membranes is extremely sensitive to the changes in pH, with a clear increase of the L_o phase domains size with the increasing pH. At the same time, lipid membranes maintained their full mobility within the whole tested pH range. The formation of domains with specific size occurs on the solid support and results from the changes in the height difference between lipids composing L_o and L_d phase under different pH of the environment. These findings demonstrate that it is possible to prepare membranes with predefined size and shape of lipid domains without any external modification of their composition. The formation of lipid domains with a specific size makes them great platforms for studying the binding of proteins, signal transduction molecules, and incorporation of membrane channels for tracking transport across the membrane.

2. Materials and methods

2.1. Materials

1,2-Dimyristoleoyl-*sn*-glycero-3-phosphocholine (14:1 PC), egg yolk sphingomyelin (SM), and cholesterol were purchased from Avanti Polar Lipids, Alabaster AL., USA. Monosialoganglioside (GM1) from bovine brain and 1,2-Dioleoyl-*sn*-glycero-3-phosphoethanolamine labeled with Atto 633 (DOPE-Atto 633), sodium hydroxide (NaOH), and hydrogen chloride (HCl) were purchased from Merck KGaA, Darmstadt, Germany. N-2-Hydroxyethyl piperazine-N'-2-ethane sulphonic acid (HEPES PUFFERAN®) was obtained from Carl Roth GmbH & Co KG, Karlsruhe, Germany. Alexa Fluor 488 conjugated with cholera toxin B subunit (CTxB 488) was obtained from Molecular Probes, Life Technologies, Grand Island, NY, USA. Calcium chloride ($CaCl_2$) was purchased from CHEMPUR®, Piekary Slaskie, Poland. Sodium chloride (NaCl) was obtained from P. P.H. STANLAB sp. j., Lublin, Poland. All the materials and reagents were used without further purification. Optical adhesive glue Norland 68 was purchased from Norland Products Inc., Cranbury, NJ, USA. The ultrapure water was obtained by using Milli-Q® Reference Water Purification System from Merck KGaA, Darmstadt, Germany.

2.2. Vesicles preparation

The SLBs were prepared by vesicles deposition on the solid support following the formerly established method [38]. In order to form multilamellar vesicles (MLV), 14:1 PC, SM, and cholesterol in chloroform solution were mixed at the molar ratio 1:1:1 with addition of 0.1 mol% of GM1 and 0.1 mol% of DOPE-Atto 633 dye to form 10 mM solution of the lipids. The lipid mixture was dried under nitrogen gas leaving a thin film of lipids deposited on the bottom of the vial. To confirm the complete evaporation of the organic solvent, the dried lipid mixture was further desiccated in a vacuum-dry chamber for at least 2 h. The lipids were resuspended in the buffer solution (10 mM HEPES and 150 mM NaCl, pH adjusted to 7.4) and exposed to four cycles of heating on the hot plate at 60 °C and vortexing. Each step of heating and vortexing was performed for 1 min. Lipid suspension containing 10 μL of multilamellar vesicles (MLVs) was distributed into new sterilized glass vials. Aliquots were stored at − 20 °C for further use and consumed within two weeks.

2.3. Vesicles characterization

Vesicles for determination of mean hydrodynamic diameter were prepared using the same composition and the same approach as for the formation of SLBs but with the final concentration of lipids 20 mM. After drying and desiccation, lipids were resuspended in 100 μL of the buffer solution (10 mM HEPES and 150 mM NaCl) with pH adjusted to the final values 2.2, 4.2, 7.2, and 9.0. Each sample was exposed to four cycles of heating on the hot plate at 60 °C and vortexing to produce multilamellar vesicles (MLVs). Subsequently, MLVs suspensions at different pH were exposed to 10 min of sonication to obtain small unilamellar vesicles (SUVs). Lipid suspensions were then diluted in the buffer of specific pH for the final lipids concentration of 0.727 mg/ml. The mean hydrodynamic diameter and polydispersity index (PDI) of the vesicles were determined from dynamic light scattering (DLS) measurements using Zetasizer Nano by Malvern Panalytical, Kassel, Germany. Prior to the measurement lipid suspensions were exposed to the ultrasound water bath for 5 min.

2.4. SLBs preparation

All buffers for SLBs preparation contained 10 mM HEPES and 150 mM NaCl. By using a suitable amount of 0.1 M HCl, pH of buffers was adjusted to the final values of 1.7, 2.2, 3.7, 4.2, 4.7, and 5.2. 0.5 M of NaOH was added to obtain buffers with pH 5.7, 6.2, 6.7, 7.2, 7.7, 8.2, 8.5, and 9.0. The adjustment was done by using pH meter ELMETRON® CP-461. Lipid vesicles were diluted 10 times by the addition of the HEPES buffer of the desired pH to obtain the final lipids concentration of 1 mM. Aliquots containing MLVs were bath-sonicated for 10 min at maximum power to generate SUVs. To prepare the solid support for lipids deposition, a thin layer of freshly cleaved mica was glued by UV-activated glue on the glass coverslip. A half-cut Eppendorf tube was placed on the top of the coverslip and sealed with silicone to create a water reservoir. 100 μL of SUVs solution was deposited on top of the mica at room temperature, followed by the addition of 2 μL of 0.1 M $CaCl_2$ solution and 8 μL of 0.01 mM CTxB 488 and allowed to settle down for 30 s before the consecutive addition of 400 μL of HEPES buffer with the desired pH. The sample was incubated for 30 min and washed by pipetting up and down with an overall of 20 ml of HEPES buffer with the corresponding pH to remove the excess, unburst vesicles. After the final wash, the Eppendorf tube was filled with the same buffer solution, closed with a glass coverslip, and sealed with medical silicone.

2.5. Confocal imaging and FRAP experiments

The confocal imaging and fluorescence recovery after photobleaching (FRAP) experiments were conducted using Zeiss LSM

710 microscope from Carl Zeiss, Jena, Germany with 40× 1.3NA oil immersion objective. Ar laser 488 nm was used for excitation of CTxB-Alexa Fluor 488. The excitation of Atto 633 was done using HeNe laser with the wavelength 633 nm. Emission was recorded at wavelength range 495–530 nm for green light channel (CTxB-Alexa Fluor 488) and 645–797 nm for red light channel (Atto 633 detection). The minimal laser powers were used to minimize photobleaching. For FRAP experiments a circular area with 10 μm diameter was bleached and the fluorescence recovery kinetics were recorded. Diffusion coefficients (D) of lipid molecules were obtained by fitting the fluorescence recovery curve following the modified Soumpasis formula (1) [39].

$$f(t) = \mathrm{a} \cdot e^{\frac{2\tau_D}{t}}\left(I_0\left(\frac{2\tau_D}{t}\right) + I_1\left(\frac{2\tau_D}{t}\right)\right) + b \tag{1}$$

where

$$\tau_D = \frac{w^2}{4D} \tag{2}$$

where a is an amplitude of the fitted recovery curve, b is the fluorescence remaining after photobleaching, w is a bleach area radius, and $I_0(t)$ and $I_1(t)$ are modified Bessel functions.

Fitting was performed for data normalized with respect to the reference intensity signal of the whole image (excluding the bleached area). The mobile fraction for the liquid disordered phase was calculated according to the formula (3).

$$R_{mobile} = \frac{\mathrm{a}}{1-b} \tag{3}$$

where a and b parameters were obtained from fitting. The extracted diffusion coefficient (D) was finally averaged from FRAP traces acquired from 10 different areas within the sample of a specific pH. This approach of determining lipids diffusion coefficient was proven widely applicable for hydrated phase-separated membranes [40] as well as for membranes of varying hydration state [41]. In the experiments we choose to excite a spot that is sufficiently large (typically 10 μm) that for all tested pH values we probed diffusivity of lipids subjected to different microenvironments and hence exhibiting different diffusivity (for instance Lo lipids moving within the Lo domains (i), those moving from Ld into Lo phase and vice versa (ii), as well as, Lo lipids moving within the Ld phase (iii)). This way we measured average diffusion coefficient of lipids associated with each of the phases. This is particularly important for the presented experiments as we intended to compare dynamics of lipids solely as a function of changing pH conditions. Choosing smaller area could lead to probing different species of lipids resulting in (potentially additional) variation in diffusion coefficient of lipids between different pH values. To determine the average size of the lipid domains and total area occupied by domains, the original confocal images were converted to black and white binary versions by adjusting the threshold of contrast in the ImageJ software [42]. At least 10 different locations were chosen from 2 different samples of the same pH, for a total of 20 images 50x50 μm each. Circularity was calculated for samples prepared at pH 4.2, 5.7, 7.2, and 9.0 using ImageJ software based on the equation (4).

$$circularity = 4\pi \frac{area}{perimeter^2} \tag{4}$$

Images were converted to black and white binary versions and smoothened, by replacing each pixel with the average of its 3 × 3 neighborhood. At least 12 images, 50 × 50 μm in size from different spots within the same sample were analyzed, each contained 12–330 domains.

3. Results and discussion

3.1. Size of lipid domains as a function of pH

SLBs were prepared from a ternary lipid mixture of 14:1 PC/SM/cholesterol in the molar ratio 1:1:1. This commonly used membrane composition is characterized by phase separation (Ld and Lo), mainly due to the difference in the fatty acid chain length between 14:1 PC and SM [43]. Ld phase is built of shorter phosphatidylcholine and cholesterol, while Lo phase is composed of saturated sphingomyelin, interleaved tightly with cholesterol. The chosen ratio 1:1:1 of 14:1 PC, SM and cholesterol has been quite well characterized in the literature regarding both structure and dynamics [44–46], allowing us to verify consistency of our membranes at neutral conditions with those studied earlier.

For labelling of the L_d phase we used fluorescent lipid, which shows high affinity and specific partitioning to disordered phase. The fluorescent probe is an Atto 633 dye covalently attached to the hydrophilic headgroup of 1,2-dioleoyl-*sn*-glycero-3-phosphoethanolamine (DOPE). Labelling of the L_o phase was done using monosialoganglioside (GM1) – a receptor of the cholera toxin subunit B (CTxB), which partitions specifically in the L_o phase [47]. The imaging of CTxB is possible due to the conjugation of CTxB with Alexa Fluor 488 dye. In general ganglioside GM1 has been shown to partition into both phases but upon binding with CTxB it preferentially localizes in the L_o phase, allowing the visualization of sphingomyelin-rich domains [44].

The confocal images of phase-separated SLBs revealed that there is an extremely strong influence of the environmental pH on the structure of lipid membranes as presented in Fig. 1. As shown in Fig. 1A the domains of L_o phase could not be resolved in the membranes labeled with both dyes and prepared in pH below 3.7. These membranes were visible as a mixture of L_o and L_d phases. As presented in Fig. 1B and C membranes prepared at pH 4.2, and 4.7 had very small domains, while in the pH range 5.7–8.2 L_o phase formed more round, and larger domains. The representative images for pH 6.2 and 7.2 are shown in Fig. 1D and E. At pH 8.5 and 9.0 domains were merging into bigger entities with areas up to tens of μm^2. Membranes prepared in these conditions contained regions with inverse domains, where L_d phase formed round domains within the L_o phase as it is shown in Figs. 1F and S1. Membranes in the whole tested pH range 1.7 – 9.0 did not show any signs of peeling off from the substrate, formation of holes, or other intrinsic defects.

Membranes containing CTxB protein for labeling did not show significant phase separation at pH below 4. To eliminate the possible impact of denaturation of CTxB protein in pH values below 4 [48], some membranes were prepared without labeling the L_o phase with CTxB-AlexaFluor 488. As shown in Fig. S2 lipid bilayers prepared at pH 2.2 (A) and 3.7 (B) without the addition of CTxB protein contained small, distinguishable domains of L_o phase, which previously were not visible under the fluorescence microscope. CTxB is a 57 kDa pentamer protein [49], which in the folded state binds up to 5 GM1 molecules, that diffuse together. Upon denaturation in pH below 4, this big complex unfolds, exposing a larger surface area with the increased number of binding sites that can hamper many lipid molecules [50]. It is thus feasible that upon denaturation of CTxB the free movement of lipids composing L_o phase and their assembly into domains is hindered. It has to be emphasized that even in harsh acidic conditions lipid bilayer without the addition of CTxB was able to reorganize its structure, which was visible as merging of lipid domains over time as depicted in Fig. S2(C, D).

The increase of the pH in the range of 1.7–9.0 causes an increase in the average domain size. To quantify the observed variation of

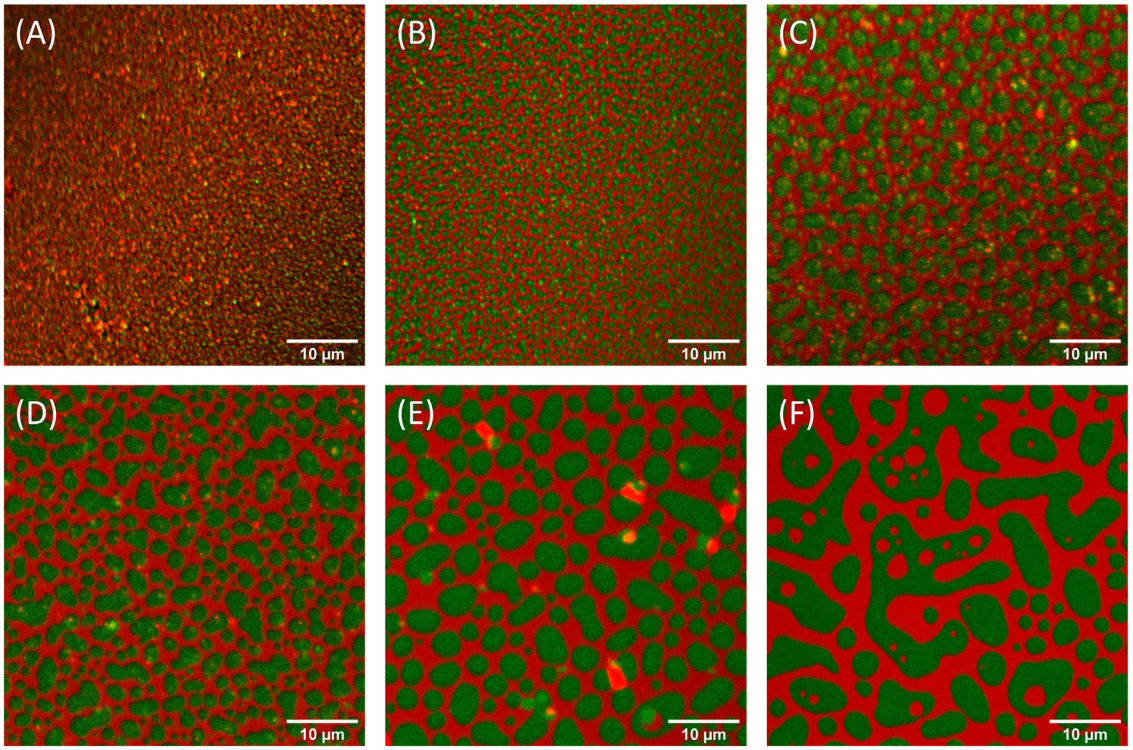

Fig. 1. Fluorescence images of supported lipid bilayers composed of 14:1 PC/SM/cholesterol and formed at pH: (A) 3.7, (B) 4.2, (C) 4.7, (D) 6.2, (E) 7.2, (F) 9.0. L_d phase was labelled with DOPE-Atto 633 (red), complex CTxB – AlexaFluor 488 marks L_o phase domains (green). The increase of the size of L_o phase domains is strongly related to the increase in the pH of the environment. (For interpretation of the references to colour in this figure legend, the reader is referred to the web version of this article.)

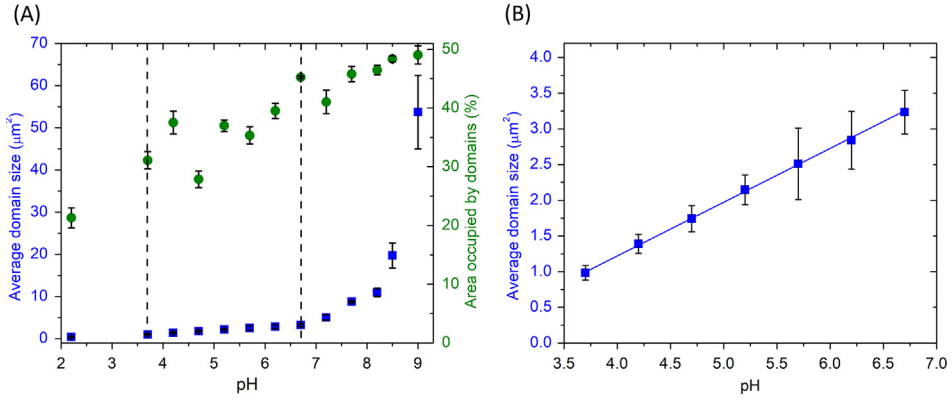

Fig. 2. (A) Average L_o domain size (marked by blue squares) and area occupied by L_o domains (green circles) as a function of pH, (B) linear dependence of the average domain size as a function of pH within the pH range 3.7 – 6.7, marked on panel (A) by two vertical, dashed lines. (For interpretation of the references to colour in this figure legend, the reader is referred to the web version of this article.)

domain sizes, lipid membranes were analyzed by using ImageJ. As presented in Fig. 2A the average L_o phase domain size for lipid bilayers prepared in pH 2.2 was 0.37 ± 0.13 μm^2, whereas for near-neutral pH 7.2 it was 5.03 ± 0.57 μm^2. The further increase of the pH led to the rapid changes in the average size of the L_o domains, which for the highest tested pH 9 was 53.71 ± 8.70 μm^2. Intriguingly, as shown in Fig. 2B the average domain size showed a linear dependence on the pH in the range of pH 3.7–6.7. In this range, the domain size increased on average by 0.38 ± 0.03 μm^2 with pH increase of 0.5. Due to the resolution limit of the confocal microscope, domains of L_o phase for the sample prepared at pH 1.7 could not be resolved.

The area occupied by domains of L_o phase was found to also increase with the increase of pH of the medium buffer. The smallest area occupied by domains was observed for pH 2.2 with the value of 22%, which was more than two times smaller than for pH 9.0, where 49% of the total image area was occupied by domains of L_o phase. It should be noted that the initial composition of membranes was the same for each tested pH condition. The decrease in the area occupied by L_o phase could be caused by the occurrence of nanodomains embedded within L_d phase at lower pH, which could not be resolved by a confocal microscope. On the other hand, it has been shown that lowering of the pH causes a decrease in the area per lipid (A_L) [51,52]. At low pH, hydrocarbon chains are more closely organized due to the decreased headgroup repulsion. The headgroup rearrangement leads to the denser packing of the lipids, which in turn causes up to 33% decrease of the area per headgroup for lipid membranes in pH 5.5 compared

with pH 9.0. It is consistent with the presented here reduction of the area occupied by domains by approximately 28% (from 1225 μm^2 to 883 μm^2) for the same values of pH as evaluated in the molecular dynamics simulation [51].

It should be noted that both acidic and basic environment can catalyze the process of lipids hydrolysis. Phosphatidylcholine can be hydrolyzed at four locations, influencing carboxy esters at *sn-1* and *sn-2* positions and phosphate ester bonds [53]. Lipid suspensions containing phosphatidylcholine have been proven to be stable for 140 h at pH 4, 7 and 10 and slowly hydrolyzed at pH 1 with a half-time of 50 h [54]. In our experiments, bilayers were monitored for no longer than 24 h. Within this time scale, only a small amount of phosphatidylcholine undergoes hydrolysis, and it can be concluded that this reaction does not influence the formation of lipid domains under both acidic and basic pH. Moreover, the hydrolysis rate reported in literature for the pH range tested in this research (1.7–9.0), would result in the formation of a negligible amount of hydrolyzed lipids, that potentially could cause a change in the architecture of the membrane.

Shaping of the lipid membranes by the formation of L_o phase domains with controlled size opens up a wide range of possibilities for potential studying of protein binding and incorporation of membrane channels that are placed specifically within the domains. However, the use of different types of proteins requires neutral or near-neutral pH of the buffer solution. To confirm the applicability of our technique for future experiments involving proteins, membrane stability was tested after the replacement of the acidic/basic buffer with a buffer of pH 7.4. The lipid membranes were prepared in pH 4.2 and 9.0 to form domains of specific size and then the liquid medium was replaced (multiple, thorough washing) with the buffer of neutral pH 7.4. After 1 h of incubation in the buffer of pH 7.4, lipid membrane domains did not change, maintaining their size and shape (see Fig. S3). The stability of the membranes was tested for 72 h. Despite the normal merging of the domains that is a natural process occurring over time, we did not observe any abnormal rearrangement of the L_o phase. It can be concluded that presented here technique of shaping of the lipid membrane allows the formation of lipid domains with a specific size in the buffer of corresponding pH, and further transfer into the medium of neutral pH for subsequent studies involving proteins and other pH sensitive molecules.

3.2. Lipids mobility under different pH conditions

To determine whether the increase of the domains size is related to the changes in mobility of the lipids at different pH values, FRAP technique was applied [55,56]. FRAP traces presenting the recovery trajectories with time after bleaching for SLBs prepared at pH 4.2, 5.7, 7.2, and 9.0 are shown in Fig. 3A. The observed recovery of the fluorescence indicated the formation of stable and continuous lipid bilayers regardless of pH conditions. In the presence of defects such as membrane perforations, curling up or detachment from the support, both fluorescence recovery as well as mobile fraction would be hampered [57]. Diffusion coefficients were determined separately for L_d and L_o phase as depicted in Fig. 3B, because of the significant differences in the mobility of the unsaturated lipids forming disordered phase and the more packed saturated lipids that belong to the ordered domains. The obtained values for the diffusion coefficient are in the range of 1.03–1.29 $\mu m^2/s$ (Fig. 3B) and are in full agreement with the work by Kataoka-Hamai, who reported that the diffusion coefficient for zwitterionic DOPC in a single component SLBs did not show significant differences (from 1.1 to 1.8 $\mu m^2/s$), when measured for pH values of 3, 4, 7.2, and 8.3 [58]. The diffusion coefficient for the sphingomyelin-rich L_o phase was 4.5–10 fold slower than for L_d phase, and varied between 0.10 $\mu m^2/s$ for pH 4.2 and 4.7, to 0.18–0.24 $\mu m^2/s$ for pH range 5.2–9.0. These results are consistent with the findings reported by Bacia et al. [47] for neutral pH condition, where depending on cholesterol concentration the diffusion coefficient between L_o and L_d phase can be 6–50-fold lower. We note here that the L_o phase is probed through CTxB molecules, which can bind to multiple GM1 molecules (from 1 to 5 units) [59]. Consequently, the diffusion coefficient measured through CTxB complex corresponds to an average diffusivity of individual lipids and also of larger lipid complexes (1–5 molecules). Hence the diffusion of L_o phase lipids is very slow and the mobile fraction is approximately around 30–40% with very little variation across the entire tested pH range. The diffusion coefficient of L_o phase lipids for SLBs prepared at pH lower than 4 could not be determined due to the plausible denaturation of the CTxB protein, which is a compound linking AlexaFluor dye with the GM1. In this case, FRAP traces could not be fitted due to the lack of fluorescence recovery, indicating that L_o phase lipids were effectively immobile. It should also be noted that lipids diffusion was not affected by the buffer replacement from pH 4.2 to 7.4 and from pH 9.0 to 7.4 (Fig. S4). Lipid membranes prepared in the buffer with specific pH can be transferred to the buffer of neutral pH without hampering the mobility of lipids.

Although changes in the pH of the environment did not affect the diffusion of the lipids in the whole range of tested pH, they influenced the mobile fraction of L_d phase. The mobile fraction for the L_d phase was increasing with the pH, showing values in the range ~70–90% with a significantly lower value of 49% for pH 3.7. The isoelectric point for a mixture of PC composed of different chain length lipids (16:0, 18:0, 18:1, 18:2, and 20:4) was found to be at pH 4.12 [60], and for SM around pH 4.01 [36]. It thus look that the reduced mobile fraction at the pH of ~3.7 is related with the isoelectric point of our membrane. Zimmermann et al. suggested that SLB composed of DOPC undergoes a charge–induced transition from a liquid-crystalline bilayer into a more ordered/gel phase bilayer at the isoelectric point [61]. At the same time they observed a gradual reduction of the diffusion coefficient below the isoelectric point. In the work by Petelska et al. they observed (supported by theoretical models) an abrupt, over a 2-fold increase of an interfacial tension for SLBs composed of PC, PS, PE and SM at their isoelectric points [36,60,62]. The observed in our data sudden reduction in the mobile fraction at the isoelectric point is in line with the mentioned, possible changes of the structural properties (phase transition and interfacial tension) in such conditions. Above the isoelectric point, the force balance between van der Waals interactions and electrostatic repulsion is maintained, which allows lipids to move freely within the bilayer, which was reflected here by the higher values of mobile fraction than for more acidic pH values [63]. However, the exact mechanism behind the observed lowering of mobile fraction at the isoelectric point remains unclear.

3.3. Rearrangement of lipid domains under different pH conditions

Based on the FRAP experiments it is clear that the formation of lipid domains with different size at different pH values is not related to the potential changes in lipids mobility. In order to determine whether variation in domain size occurs at the stage of vesicle formation, the DLS measurements were applied. The pH of the buffer in which vesicles were formed was 2.2, 4.2, 7.2, and 9.0. As shown in Fig. S5 there was no difference in the mean hydrodynamic diameter of the vesicles. Mean hydrodynamic diameter was 94 ± 3 nm, 91 ± 3 nm, 104 ± 3 nm, and 98 ± 5 nm for pH 2.2, 4.2, 7.2, and 9.0 respectively, which is a typical size for SUVs prepared by sonication method, reported in the literature [64,65]. The polydispersity index was 0.3 ± 0.04, 0.36 ± 0.09, 0.4 ± 0.03, and 0.34 ± 0.06 for pH 2.2, 4.2, 7.2, and 9.0 respectively, indicating

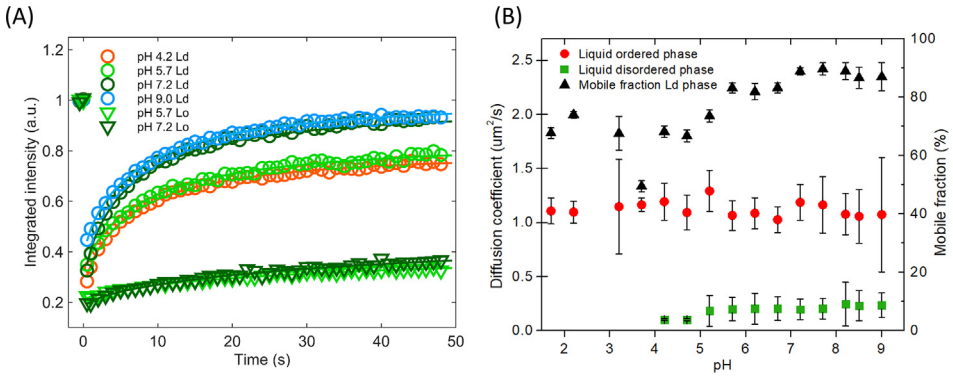

Fig. 3. (A) FRAP curves for L_d phase of SLBs prepared at pH 4.2, 5.7, 7.7 and 9.0 and for L_o phase prepared at pH 5.7 and 7.2, (B) Diffusion coefficient for L_d (red circles) and L_o (green squares) phases of SLBs and mobile fraction for L_d phase (black triangles) as a function of pH of the buffer. (For interpretation of the references to colour in this figure legend, the reader is referred to the web version of this article.)

that the obtained samples were relatively homogenous [66]. Evidently, the presence of different size of domains was not the result of the formation of bigger vesicles but must occur as a consequence of rearrangement of the lipids upon deposition onto the solid support.

To induce sample homogeneity, create the same sample thermal history in the experiment, and enable observation of the growth of the domains, samples were prepared at increased temperature, which allowed complete mixing of L_o and L_d phase lipids. Samples prepared at pH 4.2, 7.2, and 9.0 were heated during the sonication, deposition, and incubation to 65 °C, which is higher than the 14:1 PC and SM miscibility temperature [43]. The samples were imaged immediately after removing from the hot plate and domains growth was observed over time. Right after removal from the hot plate, membrane constituents were homogenously distributed, without the presence of any visible phase separation, regardless of the tested pH. The nucleation process was visible once the samples started to cool down, but the growth of domains was different for each pH as shown in Figs. 4A and S6. The beginning of the domains nucleation for the SLB prepared at pH 4.2 was visible 5 min after removal from the hot plate. However, at this time point domains were too small for quantification due to the resolution limit of the confocal microscope. After 30 min lipid domains had an average size of 0.76 ± 0.12 μm^2. Within 1 h, they doubled their size to the average value of 1.35 ± 0.13 μm^2. The domains size was checked also 3 h after removal from the hot plate and was estimated to be 1.29 ± 0.16 μm^2, indicating that the equilibration of the sample with ambient temperature and domains growth occurs within the first hour after removal from the hot plate. The same time intervals were used for checking lipid membranes prepared at pH 7.2 and 9.0. For all the samples the growth of the L_d phase occurred within the first 1 h, when domains reached the size characteristic for the tested pH and remained stable for another 2 h. The rapid merging of the domains was observed for the sample prepared at pH 9.0 as presented in supplementary Movie M1. The time-dependent evolution of the domains size for the three tested pH conditions follows the trend presented by Giocondi et al. [67] where the growth of domains prepared at neutral pH 7.4 was rapid within the first 45 min after temperature quench from 60 °C to 23 °C. It has to be emphasized that the final size of the obtained domains was different for each tested pH, even though all samples had the same starting point of a complete mixture of both phase constituents. Regardless of the tested pH, domains of L_o phase equilibrated within 1 h, obtaining exactly the same average size as when the samples were not exposed to the heating (see Fig. 2A) and did not show further significant growth for the next 2 h.

The average domain size is strongly related to the tendency of a lipid mixture to phase separate, which is regulated by three factors opposing each other. Entropy and electrostatic repulsion lead to lipid mixing and formation of small domains [68]. On the other hand, the size of domains is increased by the line tension occurring

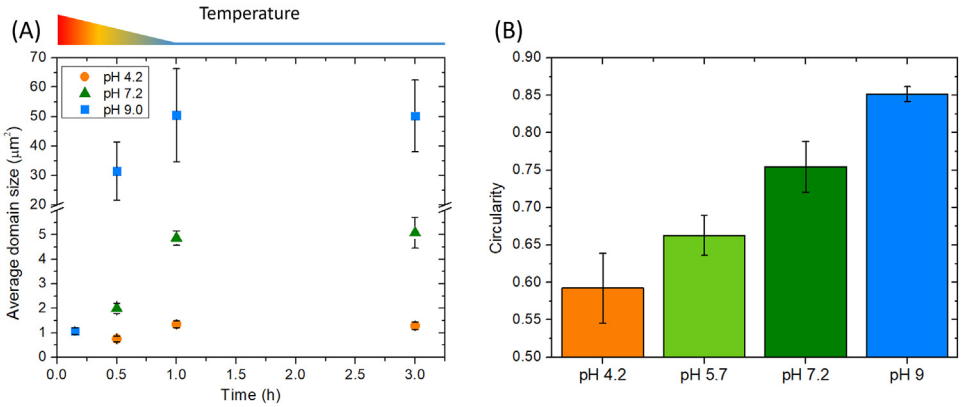

Fig. 4. (A) L_o phase domains growth as a function of time for the lipid bilayers prepared at pH 4.2, 7.2 and 9.0. Each point presenting the average domain size corresponds to the minimum of 10 images collected from 10 different areas of the lipid membrane, each analyzed image presented a minimum of 12 domains for pH 9 to approximately 330 domains for pH 4.2. (B) Circularity of the L_o domains at pH 4.2, 5.7, 7.2 and 9.0 calculated based on at least 10 different areas containing 12–330 domains each. Domains at higher pH tend to be more circular to minimize the energy at the phase boundary.

at the boundary of two phases, which tries to reduce the perimeter of the domain that is exposed to the water interface [69]. AFM studies have proven that for the ternary lipid mixture of DOPC, SM and cholesterol, L_o phase is thicker than the surrounding L_d phase [70]. This height difference leads to the phenomenon called hydrophobic mismatch, which occurs at the boundary of the two phases. The mismatch in the height is energetically unfavorable and leads to the formation of high line tension at the boundary of L_o and L_d phases. Thus, under the presence of higher line tension, the lipid membrane rearranges itself to minimize the length of the boundary at the interface of two phases, which in consequence leads to the formation of bigger domains.

According to Deplazes et al. [71] the zwitterionic lipids change their height upon pH variation. Bilayer composed of POPC, which is a zwitterionic lipid forming L_d phase, increased its thickness from 3.6 at neutral pH to 4.2 nm upon exposure to $[H_3O^+]$ ions (addition of 0.4 M of hydronium ions). The addition of $[H_3O^+]$ ions leads to the formation of acidic environment reducing the membrane fluidity and making lipid tails more straight and rigid. At low pH lipid hydrocarbon chains have higher orientational order, and a decreased headgroup repulsion [51]. Consequently, the tails of PC lipids can pack more densely, forming a more ordered state. Under acidic conditions, the height difference between protruding lipids of L_o phase and thinner L_d phase is reduced, leading to the lower hydrophobic mismatch and thus reducing the need to form bigger domains, decreasing the interfacial boundary between the two phases and enhancing their miscibility. Indeed, as presented in Fig. 4B membranes prepared in the higher pH are characterized by higher line tension, which is associated with the formation of more circular lipid domains. It is evident that the observed in this study differences in the size of domains in buffers containing different concentration of H^+ and OH^- ions are directly related to the changes in the height mismatch between L_o and L_d phases, that lead to an increase of the line tension at the phase boundary.

4. Conclusions

It has been shown that pH of the environment has a strong influence on the formation and size of the domains of L_o phase in supported lipid bilayers. The increase of pH of the environment leads to the formation of bigger L_o phase domains, exceeding the factor of 50 for pH values from 1.7 to 9.0. The increase in average L_o phase domain size is associated with an increase in the line tension and formation of rounder domains at higher pH values. Our findings are consistent with the MD simulations, which showed that unsaturated lipids take up straighter conformation under acidic pH (thickening of the L_d phase bilayer) [71]. In return this leads to the reduction of height difference between disordered and ordered phase and formation of smaller domains. On the other hand, the hydrophobic mismatch is more prominent under basic pH, which leads to the formation of bigger domains and higher line tension. We show here that the process of domains reorganization is not a result of the formation of larger vesicles but occurs at the stage of membrane establishment on the solid support. Adjustment of the environmental pH enables the control of the formation and size of domains without the introduction of mechanical boundaries that would modulate the size of lipid domains [72], use of lineactants [73], or modification of the membrane composition [74]. Given the high importance of lipid domains in many biological processes, the possibility to create these entities with a specific and repeatable size gives a wide range of new experimental opportunities. Lipid domains with fully controlled size can serve as platforms for the binding of different types of proteins such as caveolins [75], signal transduction molecules [76], and incorporation of membrane channels [77]. The diffusion of the lipid membrane proteins is normally limited by the size of the domains. Each domain can usually carry around 10 to 30 proteins [15]. The formation of bigger lipid domains gives the possibility to create binding sites for a higher amount of proteins and to observe the mutual interactions between them and other chemical complexes. It should be noted that lipid membranes prepared in different pH conditions do not lose their mobility. The measurements of the diffusion for both phases showed that although there is a significant difference in the phase separation architecture of the membranes prepared at different pH conditions, the diffusion coefficient of the lipids is not affected by pH of the environment. Finally, lipid membranes formed in specific pH do not rearrange their structure upon replacement of the basic or acidic buffer to the buffer of neutral pH. Thus presented here technique of domains shaping, enables the further studying of the lipid membranes interacting with molecules that require neutral environmental conditions.

CRediT authorship contribution statement

Emilia Krok: Conceptualization, Methodology, Validation, Writing – original draft, Visualization. **Agnieszka Batura:** Conceptualization, Investigation, Writing – original draft. **Madhurima Chattopadhyay:** Methodology, Software, Writing – review & editing. **Hanna Orlikowska:** Methodology, Writing – review & editing. **Lukasz Piatkowski:** Formal analysis, Writing – review & editing, Supervision.

Declaration of Competing Interest

The authors declare that they have no known competing financial interests or personal relationships that could have appeared to influence the work reported in this paper.

Acknowledgments

The authors acknowledge the financial support from the EMBO Installation Grant (IG 4147) and from the Ministry of Science and Higher Education of Poland in the year 2021 (Project No. 0512/SBAD/2120). L.P. acknowledges the financial support from the First TEAM Grant (POIR.04.04.00-00-5D32/18-00), provided by the Foundation for Polish Science and Opus Grant (UMO-2020/37/B/ST4/01785) from the National Science Centre, Poland. This work was financed from the budget funds allocated for science in the years 2019–2023 as a research project under the "Diamond Grant" program (Decision No. 0042/DIA/2019/48). The authors thank prof. Filip Ciesielczyk for his assistance in DLS measurements.

Appendix A. Supplementary material

Supplementary data to this article can be found online at https://doi.org/10.1016/j.molliq.2021.117907.

References

[1] S.J. Singer, G.L. Nicolson, The fluid mosaic model of the structure of cell membranes, Science 175 (4023) (1972) 720–731, https://doi.org/10.1126/science:175.4023.720.
[2] K. Simons, E. Ikonen, Functional rafts in cell membranes, Nature 387 (6633) (1997) 569–572, https://doi.org/10.1038/42408.
[3] J. Hjort Ipsen, G. Karlström, O.G. Mourtisen, H. Wennerström, M.J. Zuckermann, Phase equilibria in the phosphatidylcholine-cholesterol system, BBA – Biomembr. 905 (1) (1987) 162–172, https://doi.org/10.1016/0005-2736(87)90020-4.
[4] K. Simons, J.L. Sampaio, Membrane organization and lipid rafts, Cold Spring Harb. Perspect. Biol. 3 (10) (2011) a004697, https://doi.org/10.1101/cshperspect.a004697.
[5] C. Dart, Lipid microdomains and the regulation of ion channel function, J. Physiol. 588 (2010) 3169–3178, https://doi.org/10.1113/jphysiol.2010.191585.

[6] T.S. Tillman, M. Cascio, Effects of membrane lipids on ion channel structure and function, Cell Biochem. Biophys. 38 (2003) 161–190, https://doi.org/10.1385/CBB:38:2:161.
[7] K. Simons, D. Toomre, Lipid rafts and signal transduction, Nat. Rev. Mol. Cell Biol. 1 (1) (2000) 31–39, https://doi.org/10.1038/35036052.
[8] J.F. Hancock, Lipid rafts: Contentious only from simplistic standpoints, Nat. Rev. Mol. Cell Biol. 7 (6) (2006) 456–462, https://doi.org/10.1038/nrm1925.
[9] D.A. Brown, E. London, Functions of lipid rafts in biological membranes, Annu. Rev. Cell Dev. Biol. 14 (1) (1998) 111–136, https://doi.org/10.1146/annurev.cellbio.14.1.111.
[10] E. Ikonen, Roles of lipid rafts in membrane transport, Curr. Opin. Cell Biol. 13 (4) (2001) 470–477, https://doi.org/10.1016/S0955-0674(00)00238-6.
[11] G.R. Chichili, W. Rodgers, Cytoskeleton-membrane interactions in membrane raft structure, Cell. Mol. Life Sci. 66 (14) (2009) 2319–2328, https://doi.org/10.1007/s00018-009-0022-6.
[12] B.F. Lillemeier, J.R. Pfeiffer, Z. Surviladze, B.S. Wilson, M.M. Davis, Plasma membrane-associated proteins are clustered into islands attached to the cytoskeleton, Proc. Natl. Acad. Sci. U. S. A. 103 (50) (2006) 18992–18997, https://doi.org/10.1073/pnas.0609009103.
[13] C.M. Rosenberger, J.H. Brumell, B.B. Finlay, Microbial pathogenesis: Lipid rafts as pathogen portals, Curr. Biol. 10 (22) (2000) R823–R825, https://doi.org/10.1016/S0960-9822(00)00788-0.
[14] D.W. Zaas, M. Duncan, J.o. Rae Wright, S.N. Abraham, The role of lipid rafts in the pathogenesis of bacterial infections, Biochim. Biophys. Acta - Mol. Cell Res. 1746 (3) (2005) 305–313, https://doi.org/10.1016/j.bbamcr.2005.10.003.
[15] K. Simons, E. Ikonen, How Cells Handle Cholesterol, Science 290 (5497) (2000) 1721–1726, https://doi.org/10.1126/science:290.5497.1721.
[16] J.M. Holopainen, H.L. Brockman, R.E. Brown, P.K.J. Kinnunen, Interfacial interactions of ceramide with dimyristoylphosphatidylcholine: Impact of the N-acyl chain, Biophys. J. 80 (2) (2001) 765–775, https://doi.org/10.1016/S0006-3495(01)76056-0.
[17] R. Tero, K. Fukumoto, T. Motegi, M. Yoshida, M. Niwano, A. Hirano-Iwata, Formation of Cell Membrane Component Domains in Artificial Lipid Bilayer, Sci. Rep. 7 (2017) 1–10, https://doi.org/10.1038/s41598-017-18242-9.
[18] F. Vega Mercado, B. Maggio, N. Wilke, Modulation of the domain topography of biphasic monolayers of stearic acid and dimyristoyl phosphatidylcholine, Chem. Phys. Lipids 165 (2) (2012) 232–237, https://doi.org/10.1016/j.chemphyslip.2012.01.003.
[19] J. Zhao, J. Wu, F.A. Heberle, T.T. Mills, P. Klawitter, G. Huang, G. Costanza, G.W. Feigenson, Phase studies of model biomembranes: Complex behavior of DSPC/DOPC/Cholesterol, Biochim. Biophys. Acta - Biomembr. 1768 (11) (2007) 2764–2776, https://doi.org/10.1016/j.bbamem.2007.07.008.
[20] F.V. Mercado, B. Maggio, N. Wilke, Phase diagram of mixed monolayers of stearic acid and dimyristoylphosphatidylcholine. Effect of the acid ionization, Chem. Phys. Lipids 164 (5) (2011) 386–392, https://doi.org/10.1016/j.chemphyslip.2011.05.004.
[21] A.A. Bischof, A. Mangiarotti, N. Wilke, Searching for line active molecules on biphasic lipid monolayers, Soft Matter 11 (11) (2015) 2147–2156, https://doi.org/10.1039/C5SM00022J.
[22] A. Arnold, I. Cloutier, A.M. Ritcey, M. Auger, Temperature and pressure dependent growth and morphology of DMPC/DSPC domains studied by Brewster angle microscopy, Chem. Phys. Lipids 133 (2) (2005) 165–179, https://doi.org/10.1016/j.chemphyslip.2004.09.020.
[23] U. Bhojoo, M. Chen, S. Zou, Temperature induced lipid membrane restructuring and changes in nanomechanics, Biochim. Biophys. Acta - Biomembr. 1860 (3) (2018) 700–709, https://doi.org/10.1016/j.bbamem.2017.12.008.
[24] R.K. Paradise, M.J. Whitfield, D.A. Lauffenburger, K.J. Van Vliet, Directional cell migration in an extracellular pH gradient: A model study with an engineered cell line and primary microvascular endothelial cells, Exp. Cell Res. 319 (4) (2013) 487–497, https://doi.org/10.1016/j.yexcr.2012.11.006.
[25] E. Takahashi, D. Yamaguchi, Y. Yamaoka, A relatively small gradient of extracellular pH directs migration of MDA-MB-231 cells in vitro, Int. J. Mol. Sci. 21 (2020) 2565–2580, https://doi.org/10.3390/ijms21072565.
[26] N. Khalifat, N. Puff, S. Bonneau, J.-B. Fournier, M.I. Angelova, Membrane deformation under local pH gradient: Mimicking mitochondrial cristae dynamics, Biophys. J. 95 (10) (2008) 4924–4933, https://doi.org/10.1529/biophysj.108.136077.
[27] C.C. Yao, Z. gang Zha, Effects of incubation pH on the membrane deformation of a single living human red blood cell, Curr. Appl. Phys. 7 (2007) 11–14, https://doi.org/10.1016/j.cap.2006.11.005.
[28] C.R. Kruse, M. Singh, S. Targosinski, I. Sinha, J.A. Sørensen, E. Eriksson, K. Nuutila, The effect of pH on cell viability, cell migration, cell proliferation, wound closure, and wound reepithelialization: In vitro and in vivo study, Wound Repair Regen. 25 (2) (2017) 260–269, https://doi.org/10.1111/wrr.12526.
[29] M. Flinck, S.H. Kramer, S.F. Pedersen, Roles of pH in control of cell proliferation, Acta Physiol. 223 (3) (2018) e13068, https://doi.org/10.1111/apha.13068.
[30] A. Boussouf, S. Gaillard, Intracellular pH changes during oligodendrocyte differentiation in primary culture, J. Neurosci. Res. 59 (2000) 731–739, https://doi.org/10.1002/(SICI)1097-4547(20000315)59:6<731::AID-JNR5>3.0.CO;2-G.
[31] D. Lagadic-Gossmann, L. Huc, V. Lecureur, Alterations of intracellular pH homeostasis in apoptosis: Origins and roles, Cell Death Differ. 11 (9) (2004) 953–961, https://doi.org/10.1038/sj.cdd.4401466.
[32] S.P. Denker, D.C. Huang, J. Orlowski, H. Furthmayr, D.L. Barber, Direct binding of the Na-H exchanger NHE1 to ERM proteins regulates the cortical cytoskeleton and cell shape independently of H+ translocation, Mol. Cell. 6 (6) (2000) 1425–1436, https://doi.org/10.1016/S1097-2765(00)00139-8.
[33] M. Motizuki, S. Yokota, K. Tsurugi, Effect of low pH on organization of the actin cytoskeleton in Saccharomyces cerevisiae, Biochim. Biophys. Acta - Gen. Subj. 1780 (2) (2008) 179–184, https://doi.org/10.1016/j.bbagen.2007.10.003.
[34] K.A. White, B.K. Grillo-Hill, D.L. Barber, Cancer cell behaviors mediated by dysregulated pH dynamics at a glance, J. Cell Sci. 130 (2017) 663–669, https://doi.org/10.1242/jcs.195297.
[35] R. Zimmermann, D. Küttner, L. Renner, M. Kaufmann, J. Zitzmann, M. Müller, C. Werner, Charging and structure of zwitterionic supported bilayer lipid membranes studied by streaming current measurements, fluorescence microscopy, and attenuated total reflection Fourier transform infrared spectroscopy, Biointerphases 4 (1) (2009) 1–6, https://doi.org/10.1116/1.3082042.
[36] A.D. Petelska, Z.A. Figaszewski, pH effect of the sphingomyelin membrane interfacial tension, J. Membr. Biol. 230 (1) (2009) 11–19, https://doi.org/10.1007/s00232-009-9181-5.
[37] J. Andersson, I. Köper, Biomimetic Membranes, Compr. Nanosci. Nanotechnol. 1–5 (2019) 49–64, https://doi.org/10.1016/B978-0-12-803581-8.10447-3.
[38] S. Chiantia, N. Kahya, P. Schwille, Dehydration damage of domain-exhibiting supported bilayers: An AFM study on the protective effects of disaccharides and other stabilizing substances, Langmuir 21 (2005) 6317–6323, https://doi.org/10.1021/la050115m.
[39] D.M. Soumpasis, Theoretical analysis of fluorescence photobleaching recovery experiments, Biophys. J. 41 (1) (1983) 95–97, https://doi.org/10.1016/S0006-3495(83)84410-5.
[40] K. Sumitomo, A. Oshima, Liquid-Ordered/Liquid-Crystalline Phase Separation at a Lipid Bilayer Suspended over Microwells, Langmuir 33 (46) (2017) 13277–13283, https://doi.org/10.1021/acs.langmuir.7b02156.
[41] M. Chattopadhyay, E. Krok, H. Orlikowska, P. Schwille, H.G. Franquelim, L. Piatkowski, Hydration Layer of Only a Few Molecules Controls Lipid Mobility in Biomimetic Membranes, J. Am. Chem. Soc. 143 (36) (2021) 14551–14562, https://doi.org/10.1021/jacs.1c04314.
[42] C.A. Schneider, W.S. Rasband, K.W. Eliceiri, NIH Image to ImageJ: 25 years of image analysis, Nat. Methods 9 (7) (2012) 671–675, https://doi.org/10.1038/nmeth.2089.
[43] A.J. García-Sáez, S. Chiantia, P. Schwille, Effect of line tension on the lateral organization of lipid membranes, J. Biol. Chem. 282 (46) (2007) 33537–33544, https://doi.org/10.1074/jbc.M706162200.
[44] N. Kahya, D. Scherfeld, K. Bacia, B. Poolman, P. Schwille, Probing lipid mobility of raft-exhibiting model membranes by fluorescence correlation spectroscopy, J. Biol. Chem. 278 (30) (2003) 28109–28115, https://doi.org/10.1074/jbc.M302969200.
[45] K. Bacia, D. Scherfeld, N. Kahya, P. Schwille, Fluorescence correlation spectroscopy relates rafts in model and native membranes, Biophys. J. 87 (2) (2004) 1034–1043, https://doi.org/10.1529/biophysj.104.040519.
[46] M. Chattopadhyay, H. Orlikowska, E. Krok, L. Piatkowski, Sensing hydration of biomimetic cell membranes, Biosensors 11 (7) (2021) 241, https://doi.org/10.3390/bios11070241.
[47] K. Bacia, P. Schwille, T. Kurzchalia, Sterol structure determines the separation of phases and the curvature of the liquid-ordered phase in model membranes, Proc. Natl. Acad. Sci. U. S. A. 102 (2005) 3272–3277, https://doi.org/10.1073/pnas.0408215102.
[48] M.J.S. De Wolf, G.A.F. Van Dessel, A.R. Lagrou, H.J.J. Hilderson, W.S.H. Dierick, pH-Induced Transitions in Cholera Toxin Conformation: A Fluorescence Study, Biochemistry 26 (13) (1987) 3799–3806, https://doi.org/10.1021/bi00387a010.
[49] M. Komiazyk, M. Palczewska, I. Sitkiewicz, S. Pikula, P. Groves, Neutralization of cholera toxin by Rosaceae family plant extracts, BMC Complement. Altern. Med. 19 (2019) 1–14, https://doi.org/10.1186/s12906-019-2540-6.
[50] X.S. Sun, Soy Protein Adhesives, in: Bio-Based Polym. Compos., Academic Press, 2005, pp. 327–368, https://doi.org/10.1016/b978-012763952-9/50011-3.
[51] K. Lähdesmäki, O.H.S. Ollila, A. Koivuniemi, P.T. Kovanen, M.T. Hyvönen, Membrane simulations mimicking acidic pH reveal increased thickness and negative curvature in a bilayer consisting of lysophosphatidylcholines and free fatty acids, Biochim. Biophys. Acta 1798 (5) (2010) 938–946, https://doi.org/10.1016/j.bbamem.2010.01.020.
[52] H.A.F. Santos, D. Vila-Viçosa, V.H. Teixeira, A.M. Baptista, M. Machuqueiro, Constant-pH MD Simulations of DMPA/DMPC Lipid Bilayers, J. Chem. Theory Comput. 11 (12) (2015) 5973–5979, https://doi.org/10.1021/acs.jctc.5b00956.
[53] C.R. Kensil, E.A. Dennis, Alkaline Hydrolysis of Phospholipids in Model Membranes and the Dependence on Their State of Aggregation, Biochemistry 20 (21) (1981) 6079–6085, https://doi.org/10.1021/bi00524a025.
[54] R.J.Y. Ho, M. Schmetz, D.W. Deamer, Nonenzymatic hydrolysis of phosphatidylcholine prepared as liposomes and mixed micelles, Lipids 22 (3) (1987) 156–158, https://doi.org/10.1007/BF02537295.
[55] M. Sarkar, J.G. Koland, Fluorescence recovery after photobleaching analysis of the diffusional mobility of plasma membrane proteins: HER3 mobility in breast cancer cell membranes, in: Methods Mol. Biol., 2016, pp. 97–105. https://doi.org/10.1007/978-1-4939-3170-5_9.
[56] N.W. Goehring, D. Chowdhury, A.A. Hyman, S.W. Grill, FRAP analysis of membrane-associated proteins: Lateral diffusion and membrane-cytoplasmic exchange, Biophys. J. 99 (8) (2010) 2443–2452, https://doi.org/10.1016/j.bpj.2010.08.033.

[57] E.A.J. Reits, J.J. Neefjes, From fixed to FRAP: Measuring protein mobility and activity in living cells, Nat. Cell Biol. 3 (6) (2001) E145–E147, https://doi.org/10.1038/35078615.
[58] C. Kataoka-Hamai, M. Higuchi, Packing Density Changes of Supported Lipid Bilayers Observed by Fluorescence Microscopy and Quartz Crystal Microbalance-Dissipation, J. Phys. Chem. B 118 (37) (2014) 10934–10944, https://doi.org/10.1021/jp503905r.
[59] A.M. Kabbani, K. Raghunathan, W.I. Lencer, A.K. Kenworthy, C.V. Kelly, Structured clustering of the glycosphingolipid GM1 is required for membrane curvature induced by cholera toxin, Proc. Natl. Acad. Sci. U. S. A. 117 (26) (2020) 14978–14986, https://doi.org/10.1073/pnas.2001119117.
[60] A.D. Petelska, Z.A. Figaszewski, Effect of pH on the interfacial tension of lipid bilayer membrane, Biophys. J. 78 (2) (2000) 812–817, https://doi.org/10.1016/S0006-3495(00)76638-0.
[61] R. Zimmermann, D. Küttner, L. Renner, M. Kaufmann, C. Werner, Fluidity Modulation of Phospholipid Bilayers by Electrolyte Ions: Insights from Fluorescence Microscopy and Microslit Electrokinetic Experiments, J. Phys. Chem. A 116 (25) (2012) 6519–6525, https://doi.org/10.1021/jp212364q.
[62] A.D. Petelska, Z.A. Figaszewski, Effect of pH on the interfacial tension of bilayer lipid membrane formed from phosphatidylcholine or phosphatidylserine, Biochim. Biophys. Acta - Biomembr. 1561 (2) (2002) 135–146, https://doi.org/10.1016/S0005-2736(01)00463-1.
[63] P.S. Cremer, S.G. Boxer, Formation and Spreading of Lipid Bilayers on Planar Glass Supports, J. Phys. Chem. B 103 (13) (1999) 2554–2559, https://doi.org/10.1021/jp983996x.
[64] C.-M. Lin, C.-S. Li, Y.-J. Sheng, D.T. Wu, H.-K. Tsao, Size-dependent properties of small unilamellar vesicles formed by model lipids, Langmuir 28 (1) (2012) 689–700, https://doi.org/10.1021/la203755v.
[65] C.F. de Freitas, I.R. Calori, A.L. Tessaro, W. Caetano, N. Hioka, Rapid formation of Small Unilamellar Vesicles (SUV) through low-frequency sonication: An innovative approach, Colloids Surf. B Biointerfaces 181 (2019) 837–844.
[66] M. Danaei, M. Dehghankhold, S. Ataei, F. Hasanzadeh Davarani, R. Javanmard, A. Dokhani, S. Khorasani, M.R. Mozafari, Impact of particle size and polydispersity index on the clinical applications of lipidic nanocarrier systems, Pharmaceutics 10 (2018) 1–17, https://doi.org/10.3390/pharmaceutics10020057.
[67] M.-C. Giocondi, V. Vié, E. Lesniewska, P.-E. Milhiet, M. Zinke-Allmang, C. Le Grimellec, Phase Topology and Growth of Single Domains in Lipid Bilayers, Langmuir 17 (5) (2001) 1653–1659, https://doi.org/10.1021/la0012135.
[68] P.I. Kuzmin, S.A. Akimov, Y.A. Chizmadzhev, J. Zimmerberg, F.S. Cohen, Line tension and interaction energies of membrane rafts calculated from lipid splay and tilt, Biophys. J. 88 (2) (2005) 1120–1133, https://doi.org/10.1529/biophysj.104.048223.
[69] A. Mangiarotti, N. Wilke, Electrostatic interactions at the microscale modulate dynamics and distribution of lipids in bilayers, Soft Matter 13 (3) (2017) 686–694, https://doi.org/10.1039/C6SM01957A.
[70] D.E. Saslowsky, J. Lawrence, X. Ren, D.A. Brown, R.M. Henderson, J.M. Edwardson, Placental alkaline phosphatase is efficiently targeted to rafts in supported lipid bilayers, J. Biol. Chem. 277 (30) (2002) 26966–26970, https://doi.org/10.1074/jbc.M204669200.
[71] E. Deplazes, D. Poger, B. Cornell, C.G. Cranfield, The effect of hydronium ions on the structure of phospholipid membranes, Phys. Chem. Chem. Phys. 20 (1) (2018) 357–366, https://doi.org/10.1039/C7CP06776C.
[72] A.R. Sapuri-Butti, Q. Li, J.T. Groves, A.N. Parikh, Nonequilibrium patterns of cholesterol-rich chemical heterogenieties within single fluid supported phospholipid bilayer membranes, Langmuir. 22 (12) (2006) 5374–5384, https://doi.org/10.1021/la052248d10.1021/la052248d.s001.
[73] R. Brewster, S.A. Safran, Line active hybrid lipids determine domain size in phase separation of saturated and unsaturated lipids, Biophys. J. 98 (6) (2010) L21–L23, https://doi.org/10.1016/j.bpj.2009.11.027.
[74] S.L. Goh, J.J. Amazon, G.W. Feigenson, Toward a better raft model: Modulated phases in the four-component bilayer, DSPC/DOPC/POPC/CHOL, Biophys. J. 104 (4) (2013) 853–862, https://doi.org/10.1016/j.bpj.2013.01.003.
[75] T. Harder, K. Simons, Caveolae, DIGS, and the dynamics of sphingolipid-cholesterol microdomains, Curr. Opin. Cell Biol. 9 (4) (1997) 534–542, https://doi.org/10.1016/S0955-0674(97)80030-0.
[76] M.J. Langton, L.M. Scriven, N.H. Williams, C.A. Hunter, Triggered Release from Lipid Bilayer Vesicles by an Artificial Transmembrane Signal Transduction System, J. Am. Chem. Soc. 139 (44) (2017) 15768–15773, https://doi.org/10.1021/jacs.7b07747.
[77] J.R. Martens, K. O'Connell, M. Tamkun, Targeting of ion channels to membrane microdomains: Localization of K V channels to lipid rafts, Trends Pharmacol. Sci. 25 (1) (2004) 16–21, https://doi.org/10.1016/j.tips.2003.11.007.